Mustafa et al. *Iraqi Journal of Science, 2023, Vol. 64, No. 3, pp: 1555-1565*
DOI: 10.24996/ijs.2023.64.3.43

ISSN: 0067-2904

Image Processing Approaches as a Diagnostic Parameter to Determine Pollution by Using Satellite Imagery, Northern Iraq

Faten Azeez Mustafa[1], Almas Ahmad Khaleel[*2], Turkan Ahmad Khaleel[3]
[1]*Department of Image processing, Remote Sensing Center, Mosul University, Mosul, Iraq*
[2]*Department of Mathematics, College of Basic Education, Mosul University, Mosul, Iraq*
[3]*Department of Computer Engineering, College of Engineering, Mosul University, Mosul, Iraq*

Received: 20/4/2022 Accepted: 18/8/2022 Published: 30/3/2023

Abstract

This work highlights the estimation of the Al-Khoser River water case that disposes of its waste directly into the Tigris River within Mosul city. Furthermore, the work studies the effects of environmental and climate change and the impact of pollution resulting from waste thrown into the Al-Khoser River over the years. Al-Khoser River is located in the Northern Mesopotamia of Mosul city. This study aims to detect the polluted water area and the polluted surrounding area. Temporal remote sensing data of different Landsat generations were considered in this work, specifically Enhanced Thematic Mapper Plus of 2000 and Operational Land Imager of 2015. The study aims to measure the amount of pollution in the study area over 15 years using a supervised classification approach and other tools in ERDAS Imagine Software version 2014. Supervised classification is favored for remote sensing data processing because it contains different digital image processing methods. It is noticed by applying to preprocess and post-processing techniques adopted in the polluted section of Al-Khoser River and monitoring the changes in the objects around it. Hence, the river's water has been classified into clear water and contaminated water, which shows the impact of pollution over the years. The analysis detected a polluted area in the river that enlarged over the years 2000 to 2015 from 4.139 km² to 21.45 km², respectively. The study showed the differences in the size of objects around the river. The study concludes that daily wastes produced by the residential areas through which Al-Khoser and Tigris rivers pass would cause the polluted sections of the river to increase.

Keywords: Remote sensing data, image processing, object detection, environment pollution.

مناهج معالجة الصور كمعالج تشخيصي لتحديد التلوث باستخدام صور الاقمار الصناعية شمال العراق

فاتن عزيز مصطفى*[1] ، الماس احمد خليل[2]، توركان احمد خليل[3]
[1]مركز التحسس النائي، جامعة الموصل ، نينوى، العراق
[2]قسم الرياضيات ، كلية التربيه الاساسيه، جامعة الموصل ، نينوى، العراق
[3]قسم هندسة الحاسوب، كلية الهندسة، جامعة الموصل ، نينوى، العراق

*Email: turkan@uomosul.edu.iq

الخلاصة

يسلط هذا العمل الضوء على تأثير التغيرات البيئية والمناخية حول نهر الخوصر الذي ينبع من شمال شرق مدينة الموصل. تم استخدام بيانات الاستشعار عن بعد وبرنامج الايرداس ايماجن إصدار 2014 للإشارة إلى حالة نهر الخوصر التي تأثرت بالنفايات خلال فترة سنوات. نظرًا للدور الهام المتعلق بهذا المجال ، يتم استغلال البيانات المستشعرة عن بعد على نطاق واسع لتقدير المتغيرات البيئية ذات الصلة بصحة الإنسان. تعمل بيانات الاستشعار عن بعد الزمنية على زيادة كفاءة الكشف عن تأثير موارد المياه المتراجعة لتأثيرات الحياة البشرية على مدى سنوات مختلفة. وفقًا لذلك ، تم تنفيذ لاندسات (ETM +) لعام 2000 و (OLI) لاندسات لعام 2015 لتصنيف مساحة الغطاء الأرضي حول النهر. تم تطبيق خطوات ما قبل المعالجة وبعدها لتطبيقات معالجة الصور للحصول على الغرض من هذا العمل لرصد تباين منطقة الدراسة بسبب التلوث والأثر البيئي. وأظهرت النتائج زيادة مناطق تلوث البيئة بنهر الخُوصَر من خلال عملية التصنيف التي اظهرت اختلاف لون صنف الماء (C1) عند منطقة الخوصر بمواد اخرى ادت الى امكانية تمييز صنف آخر (C8) مما يدل على اختلاط الماء بمواد اخرى ادت الى تغير لونه الازرق او الاسود كما يظهر في المرئيات الفضائية . وهذا يعني أن 4.139 كيلومتر مربع مصنفة على أنها مياه ملوثة لعام 2000 و 21.45 كيلومتر مربع من عام 2015.

1. Introduction

Environmental change is a severe problem caused by several factors such as increasing populations, environmental pollution, land use planning, etc. Change detection has recently gained importance due to its many practical uses, such as monitoring environmental aspects, overseeing natural disasters, planning urban growth, and detecting changes in water bodies [1]. Change detection can be understood as analyzing images of a certain geographical area taken over time [2]. Thus, certain factors such as sensor calibration, sunlight, atmospheric conditions, registration strategy, and spectral characteristics of water levels that normally change with the seasons can determine the accuracy of change detection [3]. To reduce or mitigate the effect of these factors on change detection procedures, certain processing techniques, such as noise reduction, sensor calibration, and radiometric and geometric correction, can be applied [4]. The developments that remote sensing satellites gained encouraged researchers of municipal planning to use the high-spatial-resolution data provided by these satellites to study and analyze both urban areas and water surfaces. For example, in developing countries, analysis of centers of older cities and the expansion of 'edge cities' is facilitated through satellite data [5]. Despite the attempts to use satellite images in change detection, processing these images remains a challenging task that has mostly gone overlooked. Since change detection requires images captured over a prolonged duration, the atmospheric disturbance should be modeled to obtain an accurate surface reflectance of the land cover during the change detection process. Therefore, radiometric and geometric correction is essential for presenting a confident, accurate, and precise land cover change detection analysis [6]. On the other hand, the researchers took another approach to estimate water cases in the Al-Khoser River. [7] the geological aspect in evaluating the pollution resulting from heavy elements and bacteria in the Al-Khosr River. Moreover, [8] studied the physicochemical properties of the Al-Khoser River water and its importance and evaluation of protection of the environment are clean and conducive to the livelihood of aquatic animals, some of which are fish, and their health is a source of city water. At the same time, researchers [9] concentrated on the estimation spectral reflectivity of the Tigris River over the period, which is affected by the waste caused by the Al-khoser River during its entry directly within Mosul city.

2. Study Area Description

Al-Khoser River is a tributary of the Tigris River. It runs directly through the center of the ancient city of Nineveh in Northern Mesopotamia. During the reign of Sennacherib, walls were built along the banks of Al-Khoser to prevent flooding [10], as shown in Figure 1. Al-Khoser River is a small river that originates from the district of Sheikhan, specifically from Ba'Adrah. The Assyrians tried to divert the Komel River to it through bridges so that more water could reach their capital, Nineveh, but their attempts failed [8]. Before entering Mosul city, a tourist area known as the waterfalls was built on the surfaces of many detectors of geological formations. The common geological formations are the Plaspi (middle and upper Eocene), which consists mainly of calcified limestone rocks with beams from the green marl upwards, and the formation of the hole (Middle Miocene), which consists of nonsedimentary cycles regular of marl, limestone, and evaporites rock [7]. Currently, the Al-Khoser River is almost dry and used to drain sewage. It flows into the Tigris River in the center of Mosul, near the King Ghazi bridge.

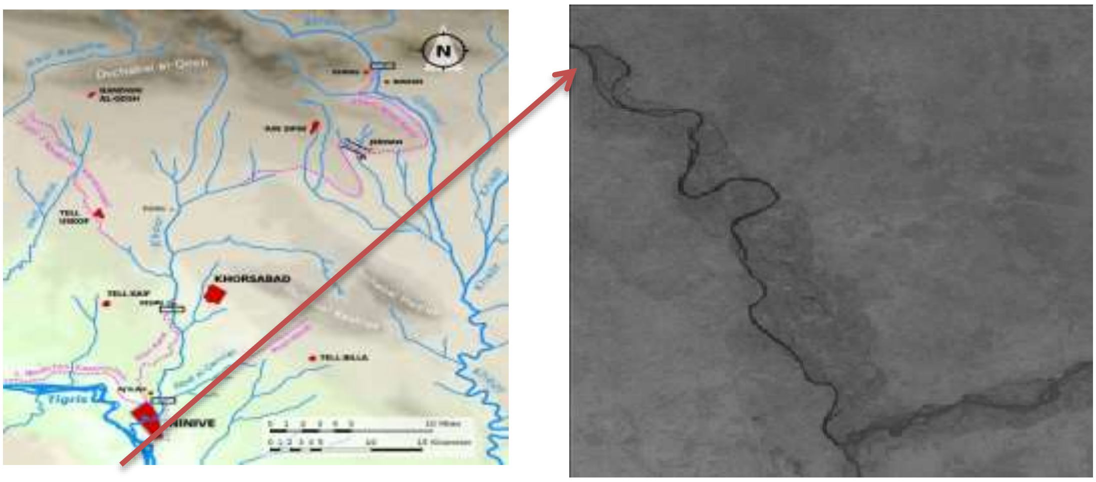

Figure 1 : Study Area Description

3. Materials and Methodology

3.1 Data Preparation

Multi-resolution and multi-temporal Enhanced Thematic Mapper Plus (ETM+) and Operational Land Imager OLI data collectors were used in this study. The data was captured in April 2000 and March 2015. The data about spectral bands used to detect the pollution near the Al-Khoser River are clarified in Table (1).

Table 1: Description of data

Landsat Type	Capture Date of data	Bands Name	Spectral resolution (µm)	Spatial resolution(m)
Landsat7ETM+	22/ April /2000	Band 1 blue	0.45–0.52	30 m
		Bnad 2 Green	0.52-0.60	30 m
		Band 4 NIR	0.77–0.90	30 m
Landsat8 OLI	20/March/2015	Band 1-ultra	0.43–0.45	30 m
		Band1 blue	0.45–0.51	30 m
		Band2 Green	0.53–0.59	30 m
		Band4 NIR	0.85–0.88	30 m

3.2 Data Processing

The study implemented sequential preprocessing steps to prepare input data and make it suitable for post-processing through different image processing techniques using ERDAS Imagine Software tools, as clarified in the flowchart shown in Figure (2).

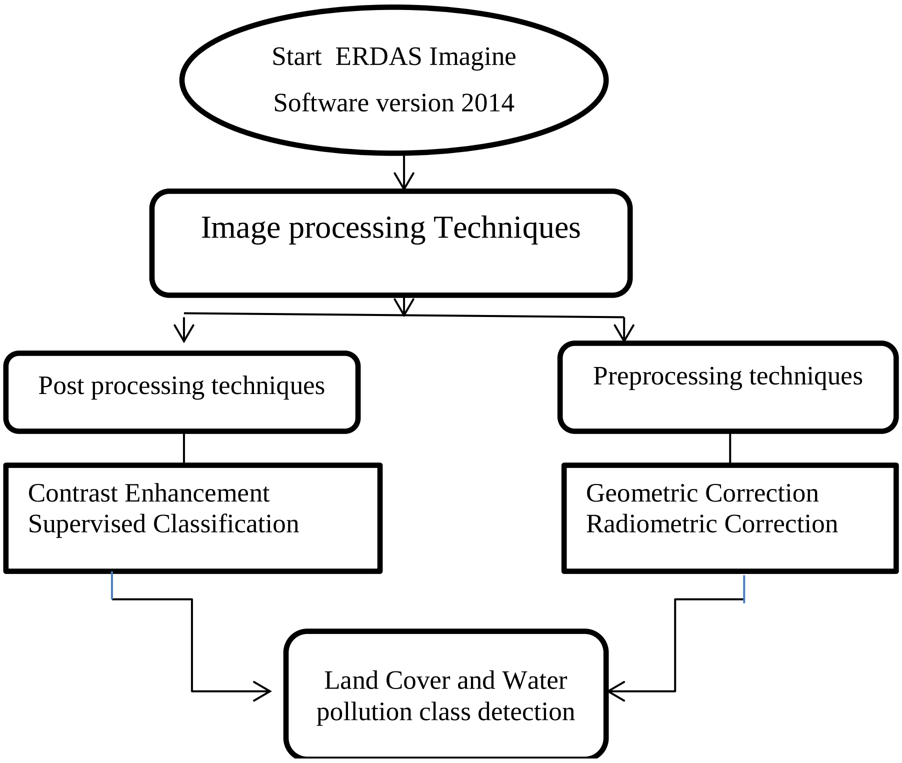

Figure 2: Flow Chart for Proposed Methdology

3.2.1 Geometric Correction

Geometric correction is adjusting the geometrical reference of satellite images to match actual coordinates on the ground as recorded on the UTM map projection system[11]. The correction steps began by displaying the images onto the projection system and marking the area under study using evenly distributed specific points taken from a digitized topographic map of similar areas. The resulting image is then resampled according to the nearest neighborhood to obtain the digital values needed to adjust the pixel locations so that the coordinates of the image and on the ground match. Nearest neighbor, bilinear interpolation, and cubic convolution are the three most common techniques used in the resampling model [12]; this requires a mathematical function as mentioned in equations 1 and 2 to process the suggested points ground control points (GCP) that are chosen between the original image and object coordinate [4]. Then polynomial transformation equation is used to solve the parameters in equations 1 and 2, as explained in equations 3 and 4, to correct the position for each pixel [13].

$$x = f1(X, Y) \quad (1)$$
$$y = f2(X, Y) \quad (2)$$

$$x = a0 + a1X + a2Y \quad (3)$$
$$y = b0 + b1X + b2Y \quad (4)$$

Where, (x,y) , image coordinate , (X,Y) is the object coordinate, and (a,b) polynomial coefficients [12].

3.2.2 Radiometric Correction:

One of the most critical stages in change detection analysis is the radiometric normalization of multi-dates images. The accuracy of the analysis depends significantly on the accuracy of the image's geometrics registration due to the difference between reflectance values recorded by the satellite sensors and the actual values on earth. Such variance in values can be attributed to the earth's surface features, sensor factors, and other external factors such as sun angle, path radiance, and atmospheric conditions [11]. The variance between the multi-date images and the actual area on the ground should undoubtedly be reduced by ensuring that the radiometric characteristics of the images captured by the sensors are comparable. This entails that the images should be adjusted to compensate for radiometric divergence if they are used in any quantitative analysis based on radiometric information, which is the case in our current research on detecting surface changes [15]. Specific algorithms are typically used to reduce the divergence and to correct any systematic or unsystematic data irregularities by using the top atmospheric correction technique to avoid noise from satellite images; this technique is based on converting the (DN) value of the image to atmospheric radiance as mentioned in equation (5)[16].

$$L\lambda = \frac{SRk \times DN}{DN\ max} \tag{5}$$

Where *SRk* is the saturation radiance of the *Kth* image (band), *DN* is the number of pixels, and *DNmax* is the total number of all pixels in the input image.

3.2.3 Enhancement

Enhancement technique refers to any adjustments made to an image to improve quality in visual or machine investigations; usually, no reference to the improvements is made [9]. This method makes an effort to improve the image such that it is both more aesthetically pleasing and understandable; the improvement could be radiometric or mathematical. The radiometric upgrade is intended to work on an image's differentiation and shading balance; at the same time, mathematical improvement looks to make spatial elements appear more transparent, for example, edges more prominent, which helps highlight extraction, image examination, and visual information [10]. Equation (6) clarified the linear contrast stretching enhancement method implemented in this work to increase the clarity of input data and extract features in an image by distributing the pixels of the image to all the brightness range values of the image (0-255) [17].

$$BVout = \left(\frac{BVin - mink}{Maxk - mink}\right).255 \tag{6}$$

BVin is the original input brightness value, the minimum mink value in the image, and maxk, the maximum value in the image, representing the full range of brightness (0-255).

Figure 2: Out images after Processing

3.2.4 Supervised Classification

Supervised classification in ERDAS Imagine Software and unsupervised classification work similarly; each is different. The first one is used training and testing data, while the second does not need training data. So the only difference between them is that ERDAS Imagine creates signature files for each class before running the classification result for supervised classification [18]; these signature files include means and covariance matrices for each class. That is to say, each band is typically dispersed and determines the likelihood that a given pixel belongs to a particular class. They are used with a classifier (often maximum likelihood) to place each pixel in the image [19]. In this study, the supervised classification was implemented to distinguish the land cover changes between two periods and to detect the pollution near that river area. The Al-khoser River enters Mosul city and passes through several residential communities that have expanded in recent years. Agricultural lands on both sides of the River and poultry fields used the river as a source for excrement disposal, making a stream for polluted water. Eight land cover classes have been recognized, as clarified in Tables 2 and 3. They are distributed on true colors images for ETM for 2000 and OLI for 2015, as shown in Figures 2 and 3. A difference throughout the period between the years was detected. By ERDAS-imagine the maximum toolbox likelihood supervised classification method implemented by the following equation (7) [20].

$$gi(x) = 1nP(\omega i) - \frac{1}{2} 1n \sum \quad i - \frac{1}{2}(x - mi)T \sum_i^{-1}(x - mi) \qquad (7)$$

Where, i = class, n: number of bands, $P(wi)$: probability for all classes, $\sum$: a determinant of the covariance matrix $\sum_i^{-1}(x - mi)$: inverse matrix, and mi: mean vector.

Table 2: Classes description for ETM image for the year 2000

Class Name	Type	Area(km^2)
C1	Uncontaminated water	188.77 km^2
C2	Agriculture land	22.818 km^2
C3	Forest	56.5326 km^2
C4	Bedrock	6.3513 km^2
C5	Barren land	36.828 km^2
C6	Marsh vegetation	177.875 km^2
C7	Grassland	32.2965 km^2
C8	Contaminated water	4.139 km^2

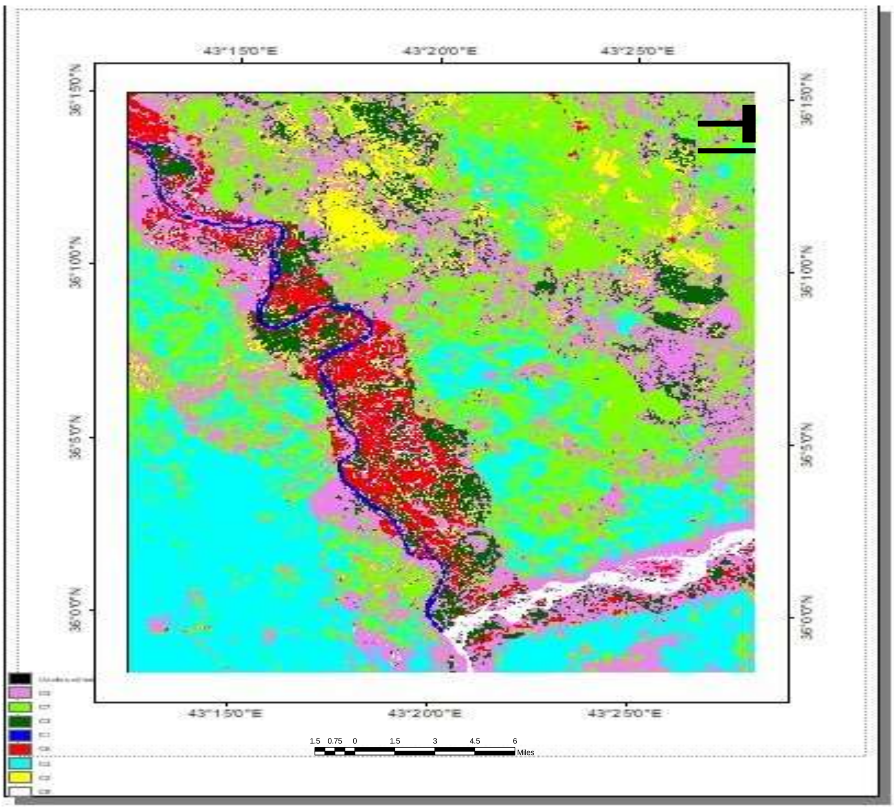

Figure -3 Supervised classification for the year of 2000 ETM bands

Table 3: Classes description for OLI image for the year 2015

Class Name	Type	Area(km^2)
C1	Uncontaminated water	155.74 km²
C2	Agriculture land	263.89 km²
C3	Forest	116.67 km²
C4	Bedrock	197.78 km²
C5	Barren land	193.53 km²
C6	Marsh vegetation	172.87 km²
C7	Grassland	277.83 km²
C8	Contaminated water	21.45 km²

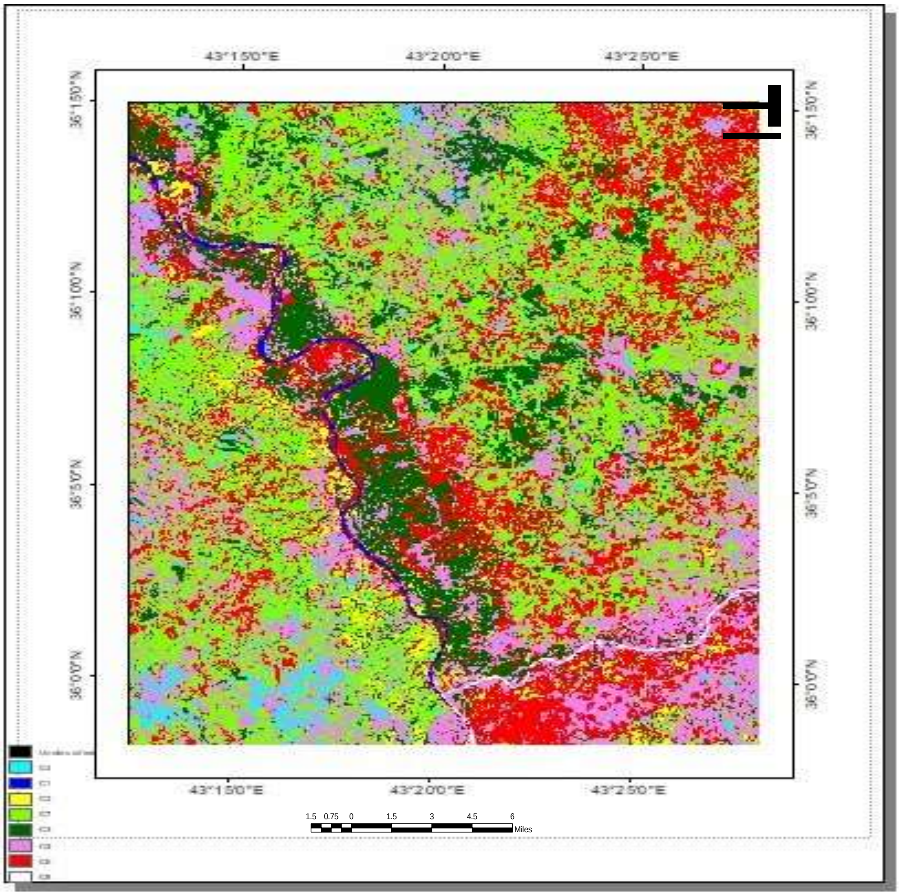

Figure -4 Supervised classification for the year 2015(OLI)

4. Results and Discussion

Surface waters and streams, in particular, are the final resort for many pollutants humans get rid of by throwing such waste in water after various uses. Service, residential, agricultural, or agricultural activity had caused high pollution for pure water, which later required an advanced processor to be helpful for the most straightforward use[21]. This work shows the impact of pollution near the Al-Khoser River as it passes in Mosul, and many outlets flow into it from many residential and industrial areas without any treatment. Consequently, due to climate change, the degree of pollution will be higher through various periods and seasons. Thus, declining rainfall in Iraq through the last years led to a decrease in water level more than 15 years ago, adding tremendous neglect in repairing water systems and sewage treatment and discharging factory and hospital waste for years. The results in Figures 3 and 4 clarified that the quantities of harmful and untreated waste dumped daily in rivers have not decreased, while freshwater is constantly and significantly decreasing. ERDAS Imagin Software and its library tools studied the case of the Al-Khoser River between the years (2000 – 2015) by utilizing satellite data to evaluate the variation in cross-sectional polluted areas and how they changed through years and seasons.

Moreover, it studies the (Figure 4) supervised classification for the year 2015 (OLI) ± 1.5, 0.75, 0 1.5 3, 4.5, and 6 Miles 8 variation of land cover features due to changes in the course of the river over the years. Tables 1 and 2 illustrate the classification category for the number of polluted areas, the features around and near the river, and how the climate variation through the years played a significant role in causing divergence of land cover objects. In addition, ERDAS Imagine Software's efficiency allows testing the work's performance by calculating the accuracy assessment as clarified in equation (8). To improve the classification efficiency and the performance of extracting features or classes, the supervised classification processing as described in equation (9), Kappa statistic value calculation was to control the samples correctly classified in exacted classes, and Kappa was near to (1) value. In contrast, those not related to their class were near to (0) value. This can be calculated using both the observed (total) and the random accuracy, as seen in equation (8). Table (4) illustrates the performance accuracy of the proposed study.

$$Overal\ accuracy = \frac{Total\ number\ of\ correct\ sample}{Total\ numbers\ of\ sample} \times 100 \tag{8}$$

$$Kappa = \left(\frac{Overal\ Accuracy - Random\ accuracy}{1 - Random\ accuracy}\right) \tag{9}$$

Table 4: The Performance of the implemented process

Input Data	Overall Accuracy %	Kappa(K^)%
ETM^+ April /2000	93.04%	0.9023%
Landsat8 March /2015	89.103%	0.864%

5. Conclusion:

Remote sensing and ERDAS Imagine Software techniques are very beneficial for extracting information about different objects of land cover such as wetland areas, urban land use patterns, and water resources. This information is significant for evaluating the environmental changes over the years. Water pollution is one of the most critical problems due to different environmental causes. This work utilizes multi-temporal remote sensing data to evaluate the polluted areas in the Al-Koser River; these areas were polluted by residential water use over the years. The study provides information to assess the structural distinction of Land Use Land Cover (LULC) patterns over the years. The results prove the efficiency of ERDAS Imagine Software and image processing tools to process remote sensing data. The results showed the overall severity of pollution caused by daily residential use and environmental degradation over 15 years, indicating that the study area, in general, is exposed to a high pollution risk from the river, as illustrated in class 8 (contaminated water) in Tables2 and 3. It prospects that this polluted area will increase in the following years due to the absence of sewage networks through which the AL-Khoser River passes. Comparing the proposed location area with other locations related to the Al-Khoser River that flows in Mosul City is necessary. The study revealed that the flow from the river throughout Mosul's city center protects the river's sustainability from contamination caused by littering and ill use of the nine surrounding areas. For future work, it is recommended to develop a study for further processing to recognize pollution quantity on water surface through applying different image processing and deep learning techniques to classify and segment water pixels in the river and recognize the type of pollutants by utilizing simulation systems.

Acknowledgments

The authors would like to thank the remote sensing center library at Mosul University for the continuous scientific support in carrying out scientific research that serves the community. Also, we appreciate the advice from our fellow geologists.

References

[1] K. Bishaw, "Application of GIS and Remote Sensing Techniques for Flood Hazard and Risk Assessment: The Case of Dugeda Bora Woreda of Oromiya Regional State, Ethiopia.," *2012 Berlin Conf. Hum. Dimens. Glob. Environ. Chang.*, pp. 1–17, 2012.

[2] B. Q. Al-abudi, M. S. Mahdi, and Y. C. Bukheet, "Study of Land Cover Changes of Baghdad Using Multi-Temporal Landsat Satellite Images," *Iraqi J. Sci.*, vol. 57, no. 3B, pp. 2146–2160, 2016.

[3] T. D. Acharya, D. H. Lee, I. T. Yang, and J. K. Lee, "Identification of water bodies in a Landsat 8 OLI image using a J48 decision tree," *Sensors (Switzerland)*, vol. 16, no. 7, pp. 1–16, 2016.

[4] L. Estrada, "Using Matlab for Expeditious Image Geometric Correction," No. figure 1, pp. 2–4.

[5] S. Voigt, T. Kemper, T. Riedlinger, R. Kiefl, K. Scholte, and H. Mehl, "Satellite image analysis for disaster and crisis-management support," *IEEE Trans. Geosci. Remote Sens.*, vol. 45, no. 6, pp. 1520–1528, 2007.

[6] D. Phiri and J. Morgenroth, "Developments in Landsat land cover classification methods: A review," *Remote Sens.*, vol. 9, no. 9, 2017.

[7] H. m J . Al-Nuaimy, M. F.O. Khattab, and M. N. Fadhel, "Adverse Impact of Al-Khoser River upon Tigris River at Outfall Area," *Iraqi Natl. J. Earth Sci.*, vol. 8, no. 1, pp. 41–55, 2008.

[8] E. Al-Sarraj, "A Study of Physiochemical Characteristics of Al- Khoser River Effluent and its Effect Upon Tigris River Quality within Mosul City," *Rafidain J. Sci.*, vol. 28, no. 3, pp. 77–89, 2019.

[9] M. F. Allawai and B. A. Ahmed, "Using GIS and remote sensing techniques to study water quality changes and spectral analysis of Tigris river within Mosul city, north of Iraq," *Iraqi Journal of Science*, vol. 60, no. 10. pp. 2300–2307, 2019.

[10] "City Profile of Mosul, Iraq," No. October 2016.

[11] T. Fernández *et al.*, "Automatic detection of landslide features with remote sensing techniques in the Betic Cordilleras (Granada, Southern Spain)," *Int. Arch. Photogramm. Remote Sens. Spat. Inf. Sci.*, vol. XXXVII, no. 8, pp. 351–356, 2008.

[12] D. S. S. Baboo and M. R. Devi, "An Analysis of Different Resampling Methods in Coimbatore, District," *Glob. J. Comput. Sci. Technol.*, vol. 10, no. 15, pp. 61–66, 2010.

[13] R. P. Gupta, R. K. Tiwari, V. Saini, and N. Srivastava, "A Simplified Approach for Interpreting Principal Component Images," *Adv. Remote Sens.*, vol. 02, no. 02, pp. 111–119, 2013.

[14] N. Panigrahi, B. K. Mohan, and G. Athithan, "Pre-processing Algorithm for Rectification of

Geometric Distortions in Satellite Images," vol. 61, no. 2, pp. 174–179, 2011.
[15] A. Behnamian *et al.*, "Semi-Automated Surface Water Detection with Synthetic Aperture Radar Data: A Wetland Case Study," *Remote Sens.*, vol. 9, no. 12, p. 1209, 2017.
[16] C. Kuhn *et al.*, "Performance of Landsat-8 and Sentinel-2 surface reflectance products for river remote sensing retrievals of chlorophyll-a and turbidity," *Remote Sens. Environ.*, vol. 224, 2019.
[17] "Art_10.1007_s12517-013-1026-y Mh.pdf." .
[18] J. I. Faraj and F. H. Mahmood, "Extraction of Vacant Lands for Baghdad City Using Two Classification Methods of Very High-Resolution Satellite Images," *Iraqi J. Sci.*, vol. 59, no. 4C, pp. 2336–2342, 2018.
[19] G. Kaplan and U. Avdan, "Object-based water body extraction model using Sentinel-2 satellite imagery," *Eur. J. Remote Sens.*, vol. 50, no. 1, 2017.
[20] X. Zhang, J. Cui, W. Wang, and C. Lin, "A study for texture feature extraction of high-resolution satellite images based on a direction measure and gray level co-occurrence matrix fusion algorithm," *Sensors (Switzerland)*, vol. 17, no. 7, 2017.
[21] S. D. Jawak, K. Kulkarni, and A. J. Luis, "A Review on Extraction of Lakes from Remotely Sensed Optical Satellite Data with a Special Focus on Cryospheric Lakes," *J*, vol. 4, no. 4, pp. 196–213, 2015.